Microstructure and abrasive wear of cobalt-based laser coatings

Mol van Otterloo, J.L.de; de Hosson, J.T.M.

Published in:
Scripta Materialia

DOI:
10.1016/S1359-6462(96)00346-6

Pergamon

Scripta Materialia, Vol. 36, No. 2, pp. 239-245, 1997
Elsevier Science Ltd

1359-6462/97 $17.00 + .00

PII S1359-6462(96)00346-6

MICROSTRUCTURE AND ABRASIVE WEAR OF COBALT-BASED LASER COATINGS

J.L. de Mol van Otterloo and J.Th.M. De Hosson
Department of Applied Physics, Materials Science Center, University of Groningen,
Zernike Complex, Nijenborgh 4, 9747 AG Groningen, The Netherlands

(Received June 18, 1996)
(Accepted August 21, 1996)

Introduction

Cobalt-based alloys are used as wear-resistant materials for hardfacing cheap steel substrates. A substantial enhancement in mechanical properties of cobalt-based superalloys is attributed to the martensitic fcc → hcp phase transformation. Alloying elements can be classified as phase modifiers (Ni and Fe stabilize fcc whereas W and Cr stabilize hcp), solid-solution strengtheners (W and Mo), which affect only the matrix, and elements that form carbides (Cr-rich M_7C_3 and $M_{23}C_6$, M = metal).

Of the different depositing techniques such as plasma spray, tungsten inert gas, oxyacetylene flame and laser cladding, the latter delivers coatings with a low dilution with the substrate material and no pores [1]. Moreover the laser cladding process has the advantage of being well controllable. This paper reports on the deposition of five different cobalt-based Stellite alloys on steel substrates by laser cladding.

Experimental

Stainless steel AISI 316 with a chemical composition listed in Table 1 is used for the substrates. The 316 substrate's dimensions are defined by a square with sides of 30 mm and a thickness of 5 mm. Stellite powders with compositions listed in Table 1 and particle size in the range of 45-125 mm are fed onto the surface with a Metco 9MP powder feeding apparatus. While cladding with the high C and W containing Stellites 1 and SF 20, the substrate material is preheated to 400°C to prevent cracking. A glass cyclone is placed between the powder feeding system and the substrate and serves as an outlet for the superfluous carrier gas to decrease the particle speed. The main advantage of this system is that the laser melt pool will hardly be disturbed by the incoming powder particles and the carrier gas. While injecting the powder particles onto the substrate, a Spectra Physics 820 transverse flow continuous wave CO_2 laser is used to fuse them together under an Ar shielding atmosphere. In this process the focal point (127 mm) of the lens is set 20 mm above the surface, resulting in a Gaussian spot diameter of 3.0 mm. The laser power (P), the laser beam sweep velocity (v_b) and the powder feeding rate (m_p) are varied in the range 430-1200 W, 2.5-10 mm/s and 16-67 mg/s, respectively. In these experiments the separation between subsequent laser tracks (s) is kept constant at 0.6 mm. After the laser treatment

TABLE 1
Chemical Composition in wt.% (*Maximum Value) and Density (ρ) in Mg/m^3 of the Used Stellite Powders and the Stainless Steel Substrate Given by the Supplier. Chemical Composition of Used Stellite Powders and Stainless Steel Substrate Given by Stellite Alloy

Stellite alloy	Co	C	B	Cr	Ni	W	Mo	Si	Fe	Mn	Cu	ρ
no. 1	48.6	2.5	-	33.0	1.0	12.5	-	1.3	1.0	0.1	-	8.69
no. 6	62.3	1.2	-	28.4	1.5	4.5	0.5	1.2	0.3	0.1	-	8.44
no. 20	46.5	2.5	-	33.0	-	18.0	-	-	-	-	-	8.78
no. 21	63.5	0.3	-	26.6	2.9	-	5.5	0.8	0.3	0.1	-	8.33
no. SF 20	42.6	1.3	3.0	19.5	12.8	14.8	-	3.1	1.5	0.5	0.9	8.39
AISI 316	-	0.08*	-	16-18	10-14	-	2-3	1.0*	63-72*	2.0*	-	8.00

the samples are cooled down from 400°C to room temperature in a 10 hour time lapse. A thorough investigation into different etchants revealed that a 4 g $KMnO_4$, 4 g NaOH and 100 ml H_2O etchant in combination with light microscopy can be exploited to reveal the carbides and the borides in the cross sections of the samples. Additionally, scanning electron microscopy (SEM) in combination with energy dispersive spectrometry (EDS) is used to calculate the volumetric dilution ratio (D_v) with the substrate [2]. Apart from these microstructural analyses, mechanical experiments are performed on the coatings. These consist of Vickers microhardness tests and abrasive wear tests. To start with, the Vickers hardness measurements are carried out with a diamond indenter using loads of 0.2 or 0.3 kg. To explore the effects of penetration of hard particles into the laser coatings, known as abrasive wear, a derived form of the ASTM G65 rubber wheel abrasive test (RWAT) is performed. Al_2O_3 particles, with grain sizes between 0.2-0.5 mm, are used as the abrasive hard material. They are fed at a rate of 2.5 g/s in between a rotating rubber wheel and the test surface. The wheel is rotating at a speed of 0.48 rot/s and it has the dimensions of Ø 67 × 9.5 mm. The test surface, which is more than 9.5 mm wide, is pressed against the rubber wheel with a load of 50 N. The experiment is terminated after a ten minutes time lapse, beyond which the wear loss is measured. The tests are performed at room temperature.

Results and Discussion

Macrohardness is the most commonly used indicator of probable abrasive wear resistance, but it is found to be unsatisfactory in the comparison of the results for the different Stellite alloys and stainless

TABLE 2
Results of the Volumetric Dilution Ratio (D_v) Measurements, Vickers Hardness (H) Tests and Wear Loss (V) in the Rubber Wheel Abrasion Experiments

Material	D_v [%]	H [GPa]	V [mm^3]
no. 1	6.8 ± 1.0	7.7 ± 0.3	8.3 ± 0.3
no. 1*	24.9 ± 2.5	6.0 ± 0.5	7.7 ± 0.3
no. 6	3.6 ± 0.3	4.98 ± 0.10	10.5 ± 0.4
no. 6*	12.0 ± 4.1	4.6 ± 0.3	8.4 ± 0.3
no. 20	19.9 ± 1.5	7.90 ± 0.10	6.8 ± 0.3
no. 20*	46.5 ± 4.2	5.7 ± 0.3	5.8 ± 0.2
no. 21	4.3 ± 0.3	4.22 ± 0.10	12.4 ± 0.5
no. 21*	3.4 ± 0.3	4.20 ± 0.05	12.4 ± 0.5
no. SF20	6.5 ± 0.5	10.7 ± 0.9	6.7 ± 0.3
no. SF20*	9.6 ± 1.5	9.3 ± 0.9	7.0 ± 0.3
AISI 316	-	1.96 ± 0.02	4.5 ± 0.2

steel is this study. The simple theory of abrasive wear is based on the concept of an abrasive particle which forms a groove whose depth varies directly with applied load and inversely with the macrohardness of the material. All of the material in this groove is assumed to be removed in a single cutting event. This leads to the well known Archard's equation:

$$\frac{V}{s} = k\frac{L}{H} \tag{1}$$

where V is the volume loss caused by wear, S is the sliding distance, L the load and H the hardness of the worn material. The wear coefficient k is a constant depending on material and system properties.

The main reason for the breakdown of this theory in the comparison of the present Stellite materials with stainless steel, as can be inferred from Table 2, is that while the hardness of the Stellites increases, the wear mechanism will gradually change from microploughing and microcutting of the stainless steel to microcutting and microcracking of the Stellites. The onset of microcracking depends on the fracture toughness (K_{Ic}) of the material. Below a critical value of K_{Ic}, at which microcracking starts to become the predominant wear mechanism, the wear resistance will increase with an increasing fracture toughness. In the present materials it should be realized that the actual fracture toughness is strongly affected by the residual stress state of the material. As for laser treated materials the residual stresses are substantial [3], a lower fracture toughness and thus wear resistance are attained. Also, the onset of microcracking depends on the applied surface pressure, and the hardness, size and acuity of the abrasive particles. As a result it has been reported that for abrasive tribosystems with less severe conditions as in the Al_2O_3 RWAT the wear resistance will solely depend on hardness [4]. One concludes that the lower wear resistance in the RWAT of the laser coated Stellite alloys is attributed to the much lower fracture toughness of these alloys compared to stainless steel.

Moreover, this argument can be used to explain the increasing wear resistance of the laser treated Stellite coatings when the volumetric dilution with the stainless steel substrates increases. To start, we have to establish the rule of mixtures between the stainless steel substrate and the Stellite coatings. Generally, there are two possible ways to approach this problem [4, 5]. The upper bound of the wear resistance is given by the inverse rule of mixtures, which is based on the assumption that the different materials (i) with volume fractions (f_i) keep the same wear resistance as when worn individually. The lower bound of the wear resistance is given by the linear rule of mixtures, which is based on the assumption that the load on the material is distributed over the different materials in proportion to their volume fractions. If we now consider the diluted coatings as two materials, i.e. stainless steel and Stellite, and assume a linear dependence between fracture toughness and volumetric dilution with the

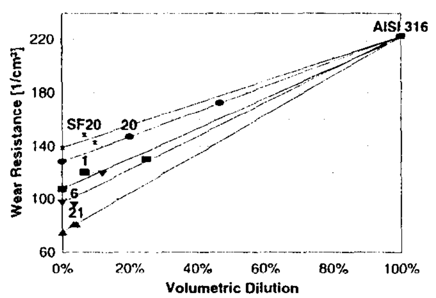

Figure 1. Wear resistance profiles as a function of the volumetric dilution ratio of the different Stellite coatings.

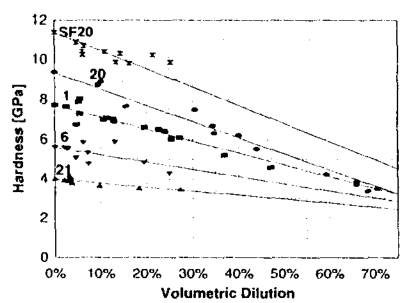

Figure 2. Hardness profiles as a function of the volumetric dilution ratio of the different Stellite coatings.

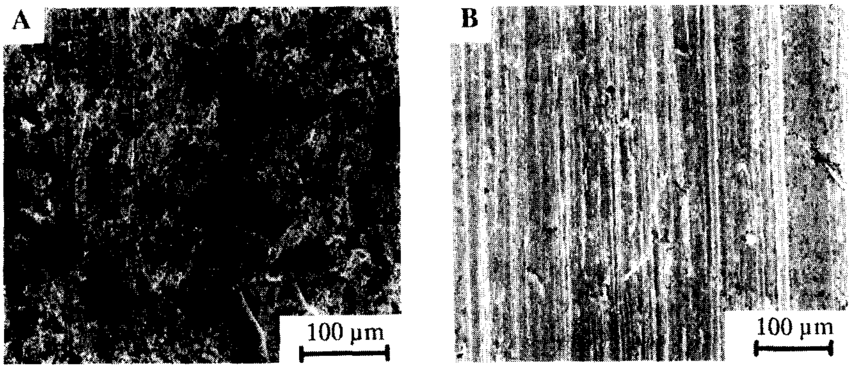

Figure 3. SEM micrograph revealing the worn surfaces of (a) stainless steel and (b) Stellite SF20.

substrate it is possible to establish the relation between the wear resistance (V^{-1}) and the different Stellites according to:

$$V^{-1} = \sum_{i=1}^{2} f_i V_i^{-1} \tag{3}$$

assuming no interaction between the stainless steel and Stellite as far as toughness is concerned [4]. Indeed, if we plot wear resistance against dilution we find linear relations (Fig. 1). Surely, the Stellites themselves are multiphase materials to which another rule of mixtures may be applicable. It is just this fact, which we will now analyze accurately.

From Fig. 1 it is clear that prudence is called for when comparing the Stellite laser coatings with each other. Dilution has such a significant effect on wear resistance that it is important to compare Stellites and their subsequent microstructures only when the dilution ratios are similar. For this reason first the intercepts of Fig. 1 are considered. To compare the abrasive wear resistance of the different Stellites with each other and hardness, we will first need to know the hardness dependence on dilution and particularly at zero dilution. The results of these experiments are plotted in Fig. 2. It can be inferred from Fig. 4 that, for a comparison within the Stellites, Archard's law does indeed hold at first sight.

As can be inferred from Fig. 2 and Table 1, the nil dilution intercepts depend on carbon content and thus carbide content. Stellites are in fact two-phase alloys in which abrading particles might alternately

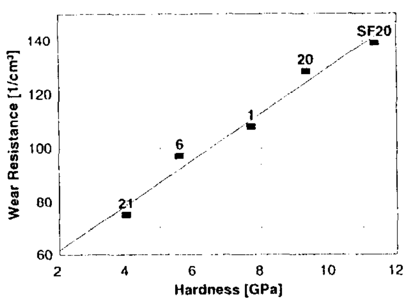

Figure 4. Wear resistance plotted as a function of hardness for the different pure Stellites, i.e. zero dilution.

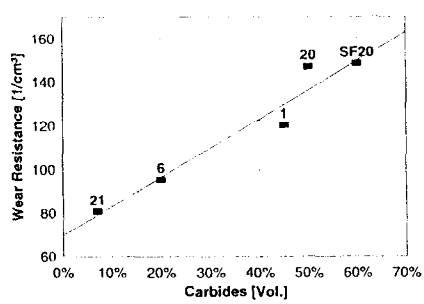

Figure 5. Wear resistance plotted as a function of volumetric carbide content for the different Stellites.

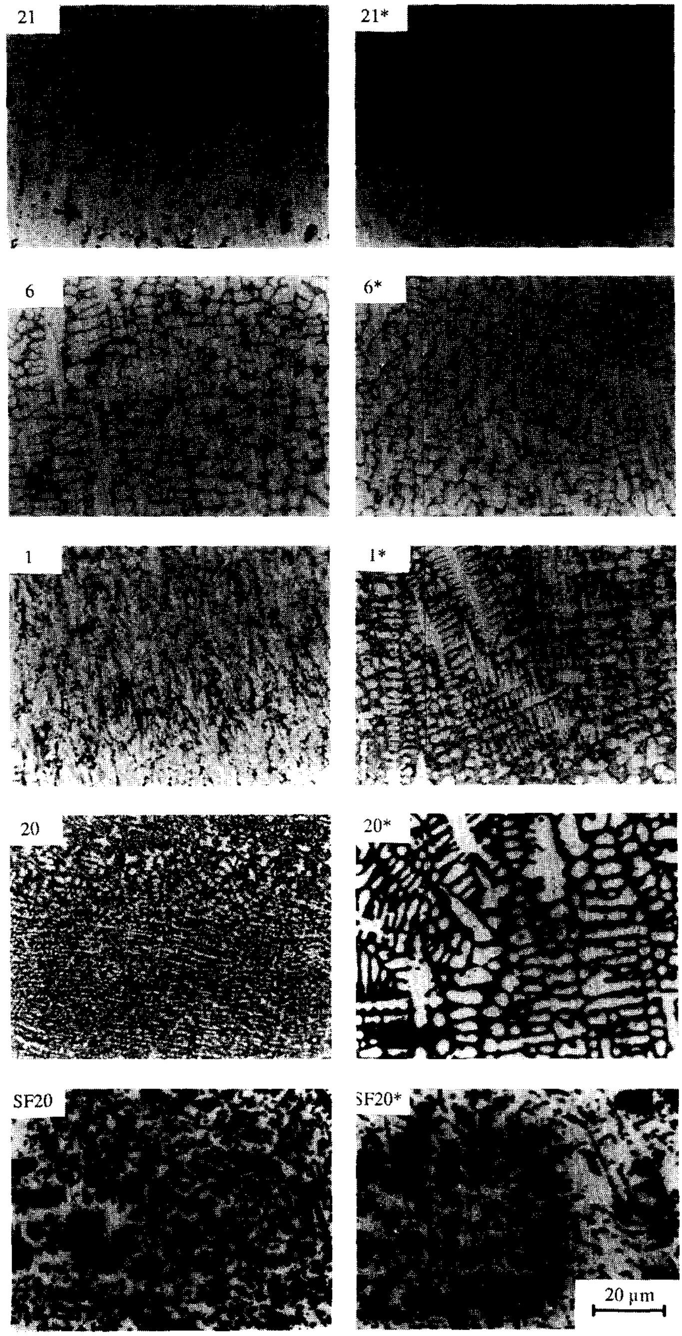

Figure 6. Equal magnification optical micrographs of etched Stellite coating cross sections as reflected in Table 2.

encounter areas of relatively soft matrix and hard carbides. In our case the matrix phase might be preferentially removed leaving the removal of the hard carbide phase the rate determining factor, because the matrix removal between the carbides is prevented by the fact that the large abrasive particles touch two adjacent carbides. The carbide diameters and inter-carbide spacings are about 1.6 ± 1.0 μm and 2.8 ± 2.3 μm on average in the different Stellites, whereas the Al_2O_3 particles are about 300 μm in diameter. Due to the relatively small size of the carbides, even when they are removed from the surface, they cannot act as abrasives themselves in the wear system described here.

Moreover, it is possible that the carbides are gradually removed by attrition of the edges. Yet, gross carbide fracture is not observed, as can be inferred from Fig. 3b, in which the worn surface of Stellite SF20 is displayed. Under these conditions one would expect alloys with higher carbide content to have lower wear rates. Thus the rate at which the matrix is removed is determined by the removal rate of the adjacent carbides. These facts and the results in Fig. 5 confirm that the Stellites obey the inverse rule of mixtures (eq. 3). The carbide content of the different Stellites were measured using the micrographs displayed in Fig. 6. In the later figure the dramatic effect of dilution on microstructure can be noticed. Especially for the cases in which the difference between dilutions is high, such as Stellite 1 and 20.

Combining Fig. 4 and 5 gives insight into the hardness of the different phases. This results in an average hardness of the matrix phase of 3.0 ± 0.8 GPa and an average hardness of the carbides of 14.3 ± 1.9 GPa. The Co matrix is harder than its pure Co constituent (1.7 GPa), due to the solid solution, Orowan looping of both the metal carbides and possible intermetallic compounds like Co_3W and dislocation-dislocation interactions. Of these different mechanisms the last is the most important matrix hardening mechanism [2]. The average hardness of the carbides can be explained by the averaging effect between the predominant carbides being present in Stellites: M_7C_3 and $M_{23}C_6$. They possess hardnesses of 17.7 and 9.9 GPa respectively [6]. Thus, to arrive at the average hardness for the carbides the average volume fraction of the carbides must be 52 and 48% respectively.

Conclusion

Notwithstanding the superior hardness of several types of Stellite laser coatings, their abrasive wear resistance in the rubber wheel abrasive test is not as good. This fact is explained by the lower fracture toughness of the Stellite laser coatings compared to stainless steel, which results in different wear mechanisms. The increase of the fracture toughness with volumetric dilution explains the better wear resistance of the diluted coatings. Moreover, the inverse rule of mixtures applies for the different Stellite laser coatings, when the Co matrix and the metal carbides are considered. In the comparison of the different Stellites it is concluded that the wear resistance is proportional to the hardness and the carbide volume content of the coatings.

Acknowledgments

The abrasive wear experiments were performed in co-operation with the Netherlands Organization for Applied Scientific Research (TNO-Apeldoorn). This work is part of the research program of the Netherlands Foundation for Technical Sciences (STW-Utrecht) and has been made possible by financial support from the Netherlands Organization for Research (NWO-The Hague) and the Foundation of Fundamental Research on Matter (FOM-Utrecht).

References

1. P.J.E. Monson and W.M. Steen, Surf. Eng. **6**, 185 (1990).
2. J.L. de Mol van Otterloo and J.Th.M. De Hosson, Microstructural Features and Mechanical Properties of a Cobalt-Based Laser Coating, Acta Mat. (1996).
3. B.A. van Brussel, H.J. Hegge, J.Th.M. De Hosson, R. Delhez, Th.H. de Keijzer and N.M. van der Pers, Scripta Met. **25**, 779 (1991).
4. K.H. Zum Gahr, Microstructure and Wear of Materials, Elsevier, Amsterdam (1987).
5. N. Axén and S. Jacobson, Wear **174**, 187 (1994).
6. W. Köster and F. Sperner, *Arch. Eisenhüttenw*. **26**, 555 (1955).